THE ASTROPHYSICAL JOURNAL, 344:991–1003, 1989 September 15

TURBULENT AND DIRECTED PLASMA MOTIONS IN SOLAR FLARES

A. FLUDRA
Mullard Space Science Laboratory, United Kingdom
J. R. LEMEN
Lockheed Palo Alto Research Laboratory
J. JAKIMIEC
Astronomical Institute, Wroclaw University, Poland
R. D. BENTLEY
Mullard Space Science Laboratory, United Kingdom
AND
J. SYLWESTER
Space Research Center, Wroclaw, Poland
Received 1988 December 2; accepted 1989 March 2

ABSTRACT

An improved method for fitting asymmetric soft X-ray line profiles from solar flares is presented. A two-component model is used where one component represents the total emission from directed upflow plasma and the other the emission from the plasma at rest. Unlike previous methods, the width of the moving component is independent from that of the stationary component. Time variations of flare plasma characteristics (i.e., temperature, emission measure of moving and stationary plasma, upflow and turbulent velocities) are derived from the Ca XIX and Fe XXV spectra recorded by the Bent Crystal Spectrometer on the *Solar Maximum Mission*. The fitting technique provides a statistical estimation for the uncertainties in the fitting parameters. The relationship between the directed and turbulent motions has been studied, and a correlation of the random and directed motions has been found in some flares with intensive plasma upflows. Mean temperatures of the upflowing and stationary plasmas are compared for the first time from ratios of calcium to iron X-ray line intensities. Finally, evidence for turbulent motions and the possibility of plasma upflow late into the decay phase is presented and discussed.

Subject headings: line profiles — Sun: flares — Sun: X-rays — turbulence

I. INTRODUCTION

The nonthermal broadening and the asymmetry of spectral line profiles during the impulsive phase of solar flares was reported by Korneev *et al.* (1979), Doschek *et al.* (1980), and Feldman *et al.* (1980). Most observations have been made in soft X-rays of the 10^7 K and hotter plasma, although similar effects have been noted in UV emissions. Since the launch of the Bent Crystal Spectrometer (BCS) experiment on the *Solar Maximum Mission* (*SMM*) in 1980 February, it has become possible to study these phenomena with better spectral and time resolution (e.g., Culhane *et al.* 1981; Antonucci *et al.* 1982; Antonucci, Gabriel, and Dennis 1984). The BCS observes the $^1S_0$–$^1P_1$ helium-like Ca XIX and Fe XXV resonance lines which can be used to study observational characteristics of the upflowing plasma. The importance of these observations is clear: the soft X-ray emission represents the thermal response of the rapidly heated flare plasma. Some authors attribute the upflowing plasma to chromospheric evaporation. Studies of the time behaviour of directed upward motions and random (turbulent) motions may constrain the interpretation for the nature and location of the heating source. For example, plasma heated by fast electrons may produce a different signature in turbulent and directed motions as compared to plasma heated by a conduction front. An extensive review of recent observations and remaining unresolved problems is given by Doschek *et al.* (1986).

The stationary and moving components of the observed soft X-ray spectra are blended and there are many transitions in the Ca XVIII–XIX and Fe XXIV–XXV line spectra. Thus, it is necessary to perform a detailed spectral synthesis to fit the observed line profiles and separate them into a component emitted by stationary plasma and a blueshifted component, emitted by plasma flowing into the flare volume. We present an improved method of fitting a two-component synthetic spectrum to the observed BCS spectra. The technique has been implemented as an automatic computer program and is an extension of the algorithm described by Lemen *et al.* (1984). The time behavior of flare parameters from flare onset and continuing to flare decay has been determined for 40 flares. Both Ca XIX and Fe XXV spectra have been analyzed. The Ca XIX results are emphasized as this channel had higher spectral resolution and better velocity resolution than the Fe XXV channel. Furthermore, Ca XIX is generally observed earlier than Fe XXV because the temperature at which the Ca XIX emission function peaks (3×10^7 K) is lower than the corresponding temperature for Fe XXV (7×10^7 K). Simultaneously recorded calcium and iron spectra have been used to compare temperatures of the stationary and moving plasma.

II. AN IMPROVED TWO-COMPONENT FITTING METHOD

a) Description

Despite the vast improvement in spectral resolution which has occurred in the recently flown instrumentation compared

to the OSO spectrometers of over a decade ago, the interpretation of the soft X-ray spectra requires careful analysis to distinguish correctly the upflowing and stationary components of the emitting plasma. The crystals in the BCS instrument provide high spectral resolution and high relative sensitivity which enables the line profiles to be determined throughout all stages of the flare. As a result, asymmetric line profiles have been observed from the rise phase of many flares typically indicating upflow velocities between 100 and 500 km s^{-1} (Antonucci *et al.* 1982). These studies have generally been made using the emission from the $^1S_0$–$^1P_1$ helium-like resonance lines in Ca XIX and Fe XXV. Antonucci *et al.* (1982, 1984) attempted a two-component fit to the observed spectra. This is an instructive approach which can reveal the relationship between the moving and stationary plasmas, although, the actual emitting plasma may very well have a broad distribution of velocities (Cheng *et al.* 1983; Pallavicini *et al.* 1983).

The profile of an unblended line emitted by a plasma at rest is represented by a Gaussian with total intensity I_S, full width at half-maximum intensity (FWHM) $\delta\lambda_S$ and wavelength λ_S. The line width is caused by the thermal and nonthermal (turbulent) motions of the emitting ions. The profile of the blueshifted component cannot generally be determined independently because it is usually blended with the stationary component. Based on numerical simulations (Mewe *et al.* 1985) we assume that the blueshifted component can also be approximated by a Gaussian profile with total intensity I_B, width (FWHM) $\delta\lambda_B$, and wavelength λ_B. The line width of the blueshifted component will generally be different from that of the stationary component because: (1) a single profile is assumed to represent a range of upflow velocities, (2) nonthermal random motions may develop in the upflowing plasma, and (3) in complex flares the upflows of plasma may take place simultaneously in different loops, with a different distribution of velocities along each loop; since the BCS 6′ (FWHM) collimator limits the field of view to a single active region but provides no spatial resolution, the emission from all emitting loops will be summed together in the resulting spectra.

To fit a spectrum containing a stationary and blueshifted component it is necessary to vary six parameters in addition to the background level. However, because the blueshifted and stationary components are usually blended, it is not always possible to find a unique solution for all six parameters. The ambiguity increases when the signal-to-noise ratio is poor. When the fitting problem is over specified, an assumption must be made to reduce the number of free parameters. A straightforward approach adopted by Antonucci *et al.* (1982) is to assume equal line widths for the blueshifted and stationary components: $\delta\lambda_S = \delta\lambda_B$. However, we found that spectra which had a well pronounced blueshifted component were not well fitted using this simple assumption. Therefore, we proposed a different constraint: namely, that the Doppler width of the blueshifted component be made proportional to its wavelength shift relative to the stationary component:

$$\Delta\lambda_B = K \times (\lambda_S - \lambda_B) \qquad (1)$$

where K is a constant of order unity and $\Delta\lambda_B = \delta\lambda_B/[2(\ln 2)^{1/2}]$. This is equivalent to assuming that the width of the blueshifted profile is proportional to the velocity of the directed motions. We determine (see discussion below) that the choice $K = 1$ adequately represents the Ca XIX and Fe XXV spectra in most cases. A further constraint is imposed on the width of the blueshifted component so that it cannot be smaller than the thermal width of the line.

To illustrate the difference between the two assumptions we calculate a two-Voigt profile model in a limited wavelength region (3.17–3.18 Å) near the Ca XIX resonance line (Fig. 1). The composite spectra (*solid curve*) assuming $\Delta\lambda_B = \lambda_S - \lambda_B$ are shown in Figures 1*a* and 1*c* for the upflow velocities 250 and 350 km s^{-1}, respectively, and the intensity ratio of the two components equal to 0.5. To compare, we plot in Figures 1*b* and 1*d* synthetic two-component spectra assuming $\delta\lambda_B = \delta\lambda_S$ and generated with the same velocities, intensity ratios, and stationary component line widths as were assumed in Figures 1*a* and 1*c*. In both cases the spectra have been folded through the BCS Ca XIX spectrometer wavelength response function. Broken lines represent the blueshifted and stationary components. The fitting technique illustrated in Figures 1*a* and 1*c* will be adopted throughout the rest of this paper.

Because of the numerous line blends present in the Ca XVIII–XIX and Fe XXIV–XXV spectra, it is necessary to synthesize the entire spectrum in order to obtain a good estimate of the plasma parameters. For an isothermal plasma the intensity of a line is given by

$$I_i(T_e) = \frac{n(Z)}{n(\mathrm{H})}\frac{n(\mathrm{H})}{n_e} G_i(T_e) \int n_e^2\, dV\,, \qquad (2)$$

where n_e is the electron density, $n(\mathrm{H})$ is the number of hydrogen atoms, $n(Z)/n(\mathrm{H})$ is the elemental abundance, $G_i(T_e)$ is a function containing all the temperature dependent factors including the effective excitation rate coefficients and the ionization balance for line i, and dV is the volume of the emitting plasma. Here we assume $n(\mathrm{H})/n_e = 0.85$, $n(\mathrm{Ca})/n(\mathrm{H}) = 3.98 \times 10^{-6}$, and $n(\mathrm{Fe})/n(\mathrm{H}) = 3.98 \times 10^{-5}$. The integral

$$\int n_e^2\, dV$$

is often referred to as the emission measure (EM).

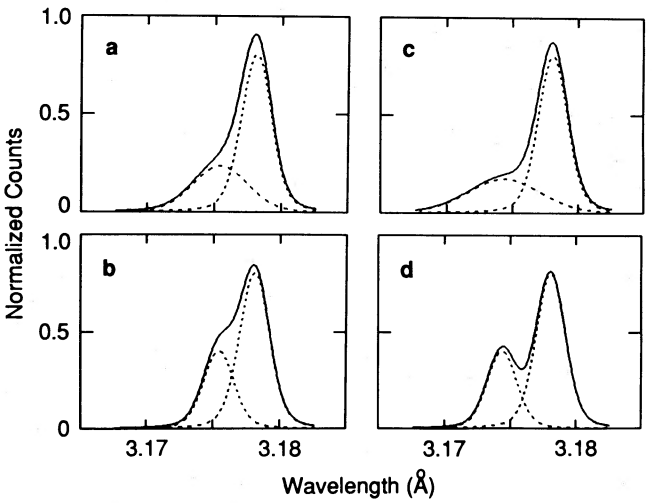

FIG. 1.—Synthetic Ca XIX resonance line spectra folded through the BCS spectrometer wavelength response function. The moving and stationary components are shown as dashed lines, the composite spectra are shown as solid lines. Panels *a* and *c* illustrate the assumption $\Delta\lambda_B = \lambda_S - \lambda_B$. Panels *b* and *d* illustrate the assumption that the upflow and stationary components have the same line widths: $\delta\lambda_S = \delta\lambda_B$. The upflow velocities are $v = 250$ km s^{-1} in panels *a* and *b* and 350 km s^{-1} in panels *c* and *d*. The intensity ratio of moving to stationary component is 0.5 in all cases.

The average electron temperature of a calcium- or iron-emitting plasma may be estimated from the intensity ratio of the lithium-like dielectronic satellite k in Ca XVIII or j in Fe XXIV to the resonance line w, in the notation of Gabriel (1972). The intensity ratio is independent of electron density or ionization balance and varies approximately as T_e^{-1}. This technique has been discussed by several authors (e.g., Bely-Dubau *et al.* 1982; Lemen *et al.* 1984). To compute a two-component spectrum consisting of the emission from plasma at rest (stationary) and upflowing plasma, it is necessary to specify the electron temperature and emission measures for the two components, the velocity of the second component and the background, or a total of six parameters. In practice, the blue-shifted components of the dielectronic satellite lines k and j are too weak to be reliably separated in the BCS spectra. Therefore, it is not possible to independently estimate the temperatures of the two components using this technique, and thus, we assume that the electron temperatures of the two components are equal: T_e(blueshifted) = T_e(stationary). The consequences of this assumption and a method to verify it are discussed in § III*e*.

Two-component fits are performed to the BCS Ca XVIII–XIX and Fe XXIV–XXV spectra by first computing the theoretical spectra corresponding to the sum of the stationary and upflowing plasmas. To compute the theoretical Ca XVIII–XIX spectrum we use the rates given by Bely-Dubau *et al.* (1982), the wavelengths of Hata and Grant (1984), and the ionization balance of Jacobs *et al.* (1980). For Fe XXIV–XXV spectra we use the ionization balance of Jacobs *et al.* (1977) and the data described by Lemen *et al.* (1984) and references therein. We note that the presence of high-n dielectronic satellites which are blended with the resonance line are automatically accounted for in this fitting procedure. An example of a two-component fit to a Ca XIX rise phase spectrum is shown in Figure 2. The observed spectrum, shown in histogram format, was acquired during an M4 flare which occurred on 1980 April 8. This flare has been studied by others, most recently by Bruner *et al.* (1988 and references therein) who used *P78-1*, *SMM*, and microwave data to study the time evolution of the source volumes. Here we will concern ourselves mainly with the determination of plasma motions from the soft X-ray spectra. The sum of the two-component fit is shown as a solid curve and the stationary component is shown as a dashed curve. For improved clarity the second component is not shown separately. In the case of the illustrated spectrum, the fit yielded an upflow velocity of 280 ± 20 km s^{-1}.

The two-component theoretical spectrum in Figure 2 has been convolved with the BCS instrument's wavelength and sensitivity functions. The wavelength response function is characterized by a Voigt profile where the Lorentzian width corresponds to the crystal rocking curve and the Gaussian width corresponds to the electronic spectral binning uncertainty in addition to the effect of the Doppler motions of the emitting ions. Parameters for the BCS wavelength response function are given in Table 1.

The convolved spectrum is compared to the observed spectrum by computing the statistic

$$\chi^2 = \sum_{i=1}^{N} \frac{(D_i - y_i)^2}{D_i}, \tag{3}$$

where D_i and y_i are number of observed and computed counts in wavelength bin i of the spectrum and N is the number of bins included in the comparison. Only wavelength regions around the resonance line w and the dielectronic satellite line k are included in the fitting algorithm and N (usually equal to 53 for Ca spectra) is therefore smaller than the total number of bins in the BCS wavelength channels. The intersystem lines (x and y) and certain $n = 2$ satellite lines are omitted because the theoretical line strengths do not appear to accurately predict their intensities. All free parameters are adjusted simulta-

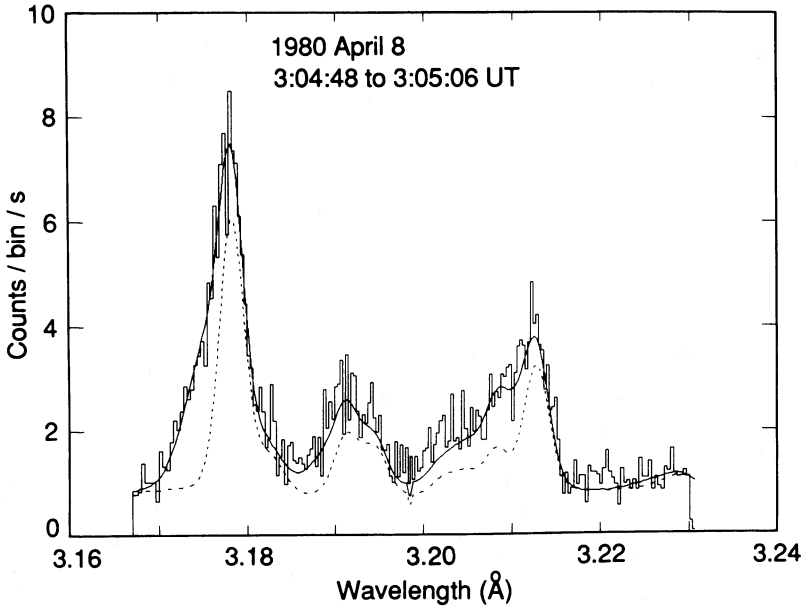

FIG. 2.—The Ca XVIII–XIX spectrum from the 1980 April 8 flare at 3:04:57 UT (integration time = 18 s) showing the most pronounced blueshifted component. The data is shown as a histogram and the best fitted spectrum is shown as a solid curve. The fitted spectrum was computed using the two-component model with $K = 1$. The stationary component is shown separately as a dashed curve. The spectral fitting yielded an upflow velocity of $v_U = 280 \pm 20$ km s^{-1} and the intensity ratio of the blueshifted to stationary component is 0.7 ± 0.16.

TABLE 1

CHARACTERISTICS OF *SMM-BCS*: CA XIX AND FE XXV

Ion	Channel	Wavelength range (Å)	Crystal	$2d$[a] (Å)	$\delta\lambda_G$[b] (mÅ)	$\delta\lambda_L$[c] (mÅ)	λ_0[d] (Å)	A_E[e] (cm^2)
Ca XVIII–XIX	1	3.165–3.231	Ge 220	4.000	0.527	0.612	3.1781	2.4×10^{-2}
Fe XXII–XXV	4	1.840–1.894	Ge 422	2.310	0.430	0.066	1.8509	5.9×10^{-3}

[a] d is the interplanar spacing of the crystal.
[b] $\delta\lambda_G$ is the FWHM of the electronic spectral binning uncertainty (Gaussian).
[c] $\delta\lambda_L$ is the FWHM of the crystal rocking curve (Lorentzian).
[d] λ_0 is the helium-like resonance line wavelength.
[e] The spectrometer effective area at λ_0. Although the sensitivity is approximately constant over the wavelength range of the individual channels, the effective areas (A_E) were multiplied by the following wavelength-dependent factors:

$$1 + 1.4290(\lambda - 3.1781) + 1.5121(\lambda - 3.1781)^2 , \quad \text{for calcium ,}$$

$$1 + 2.5809(\lambda - 1.8509) + 4.1383(\lambda - 1.8509)^2 , \quad \text{for iron .}$$

neously to minimize χ^2, using a gradient search and parabolic expansion algorithm.

b) *Choosing the Value of K*

Three flares with intensive upflows of plasma were studied to determine the best value of K, the proportionality constant in equation (1) between the Doppler width and wavelength shift of the blueshifted component. The procedure was to choose a value for K and then allow all other parameters to vary in order to determine minimum value of χ^2 (eq. [3]). This was repeated for different values of K. The values of $\chi^2_\nu = \chi^2(K)/\nu$, where $\nu = 47$ is the number of degrees of freedom, are summarized in Table 2 for several calcium spectra. The minimum value of χ^2_ν corresponds to $K = 0.3$ in one spectrum, $K = 0.6$ in two spectra, and to $K \geq 0.8$ in 12 other spectra presented in Table 2 for the three flares studied.

The statistical significance of the above results for K can be evaluated according to the procedure given by Avni (1976) and Cash (1976). For the case of one parameter, K, the statistic $\Delta\chi^2 = \chi^2(K) - \chi^2_{\min}$ must be considered, where $\chi^2_{\min}$ is the minimum value among all $\chi^2(K)$ values. This statistic has a χ^2 distribution with 1 degree of freedom, hence the critical value of this statistic, at the 0.05 significance level, is 3.84, or ~ 0.08 when normalized by ν. Thus, for example, for the first spectrum of the 1980 April 8 flare, at 3:04:22 UT, values of K between 0.3 and 1.2 are within the confidence interval. In this case, it is not possible to determine uniquely the width of the blueshifted component on the basis of χ^2, but a rather wide range of values is permitted statistically. This is true for almost all spectra. The confidence interval for K shifts in some spectra toward greater values of K. For example, the range of K becomes ~ 0.95–2.0 for the 1980 June 25, 15:52:14 UT, spectrum and 0.6–3.0 for the 1980 April 8, 3:05:13 UT, spectrum, for the 0.05 significance level. This reflects our earlier assertion that the problem is overspecified. Although the above estimates are only approximate, they are able to demonstrate that it is possible to choose a constant value for K that belongs to all confidence intervals for most spectra in different flares. On the basis of the results in Table 2 we have assumed $K = 1$ for all flares. For consistency with the calcium spectra we assume $K = 1$ for iron spectra as well.

TABLE 2

MINIMUM VALUES OF χ^2 OBTAINED FROM CA XVIII–XIX SPECTRA FOR DIFFERENT VALUES OF $K = \Delta\lambda_B/(\lambda_S - \lambda_B)$

TIME (UT)	VALUES OF K						
	0.3	0.6	0.8	1.0	1.2	2.0	3.0
1980 October 14							
6:01:46	2.30	1.41	1.33	1.33	1.33	1.31	1.32
6:03:16	4.39	2.05	1.75	1.69	1.68	1.71	2.01
6:04:01	4.12	2.41	2.13	2.04	1.99	2.07	2.34
6:05:53	7.00	3.42	2.93	2.79	2.73	2.71	2.83
1980 April 8							
3:04:22	1.09	1.04	1.04	1.05	1.05	1.22	1.32
3:04:40	1.03	1.06	1.10	1.13	1.14	1.15	1.14
3:04:57	1.93	1.30	1.18	1.14	1.14	2.13	2.55
3:05:13	1.40	1.01	0.97	0.99	0.99	0.98	0.98
3:05:28	2.57	1.47	1.29	1.24	1.22	1.30	1.46
3:05:58	1.76	1.12	1.00	0.95	0.93	0.90	0.96
3:06:13	3.21	1.76	1.35	1.19	1.15	1.21	1.52
1980 June 25							
15:51:29.....	1.82	1.55	1.57	1.61	1.63	1.66	1.64
15:51:52.....	2.93	2.02	1.90	1.89	1.91	1.87	1.84
15:52:14.....	4.13	2.31	1.94	1.79	1.75	1.74	1.90
15:52:37.....	2.87	1.96	1.85	1.84	1.85	1.89	1.94

We do not claim that $K = 1$ necessarily represents the true solution of the problem. As demonstrated in Table 2 and discussed above, χ^2 varies slowly with K in some spectra (e.g., only by 0.02 for K between 0.6 and 3.0 for 1980 April 8 flare at 3:05:13 UT). However, the proposed model (eq. [1]) with $K = 1$ is a solution that provides statistically satisfactory results and can be applied to a large number of spectra automatically with a computer.

The effect of the choice of the value for K is demonstrated in Figure 3. The two synthetic spectra, corresponding to $K = 0.8$ and $K = 2$ were fitted to the same observed spectrum for the flare of 1980 June 25 at 15:51:52 UT. The stationary components are represented by a dashed line. Although the values of χ^2/ν differ only by 0.03 and the total fits (*solid curve*) are similar, the corresponding ratios of emission measures of the moving to stationary component EM_B/EM_S are 0.40 ± 0.08 and 1.07 ± 0.20; the upflow velocities are 270 ± 15 and 146 ± 12 km s^{-1}, respectively. In general, it was determined that a reduction in K from 1.0 to 0.6—so by even a smaller amount than in the above example—causes the following systematic trends, however, fits to the spectra may not be statistically acceptable in all cases: the mean upflow velocity increases by 40–100 km s^{-1}; the emission measure of the stationary component (EM_S) increases by 5%–10%, the emission measure of the blueshifted component (EM_B) decreases by 30%–50%, the ratio of the FWHM width of the blueshifted component ($\delta\lambda_B$) to the FWHM width of the stationary com-

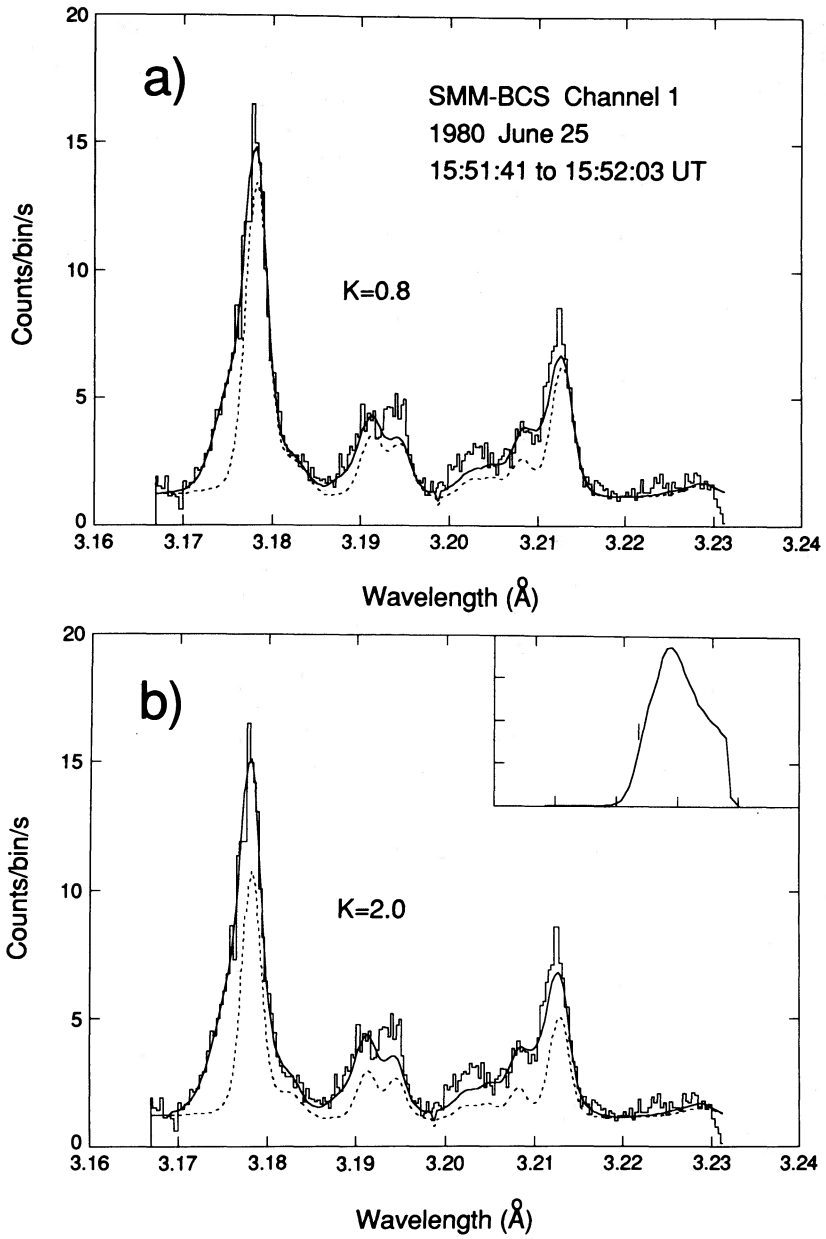

FIG. 3.—Two synthetic spectra fitted to the same spectrum observed for the 1980 June 25 flare, at 15:51:52 UT (integration time = 22.5 s). They illustrate the difference between the stationary components (*dashed lines*) obtained with the assumption $\Delta\lambda_B = K(\lambda_S - \lambda_B)$ for $K = 0.8$ (*a*) and $K = 2$ (*b*). The insert on (*b*) shows a schematic of the total light curve and the arrow marks the time when the spectrum was obtained.

ponent ($\delta\lambda_S$) decreases from ~ 2.0 to ~ 1.2. However, the change of K usually does not effect the time behavior of a given parameter throughout a flare.

III. RESULTS

We have analyzed 40 flares observed by the *SMM*–BCS during 1980, 1984, and 1985. Table 3 contains the times of these flares and several characterizing quantities. The rise phase was not observed for five flares, 12 flares showed only a very weak asymmetry of line profiles, but the 23 remaining flares showed the presence of plasma upflow during the impulsive phase. For six of these 23 flares the very early stage of flare heating is observed: in these flares the upflow velocity is observed to increase at the flare beginning. For all other flares the upflow velocity has already reached its maximum observed value (~ 300–350 km s^{-1}) by the time the spectra have become statistically significant, which in the case of the *SMM*–BCS is when the total number of counts recorded (integrated over the observing interval) has reached ~ 750–1000 counts. For some flares the upflow of plasma can be studied in spectra with a lower number of recorded photons, but the spectral fitting is less certain.

a) Plasma Upflow Characteristics

The intensity ratio of the blueshifted component to the stationary component is typically observed to vary between ~ 0.2 and 0.35. For most flares the maximum value of this ratio is ~ 0.3–0.4 but in a few cases reaches 0.6–0.7. Numerical models

TABLE 3

LIST OF STUDIED FLARES

Date	Time	Peak Ca (count s^{-1})	Active Region	Coordinates	*GOES* Class	Comments
1980 Apr 7	01:09	1520	2372	N10 E03	M4.0	[a]
1980 Apr 7	05:41	3470	2372	N12 E01	M8.0	[a]
1980 Apr 8	03:07	1780	2372	N12 W13	M4.0	[b]
1980 Apr 30	20:25	810	2396	S13 W90	M2.2	[c, d]
1980 May 7	14:57	385	2418	S22 W12	C7.0	
1980 May 9	07:14	4000	2418	S21 W32	M7.0	
1980 May 21	21:05	4900	2456	S14 W15	X1.4	
1980 Jun 25	15:54	1870	2522	S29 W28	M4.8	[b]
1980 Jun 29	02:38	1380	2522	S24 W90	M3.6	[c, d]
1980 Jun 29	10:43	2070	2522	S24 W90	M4.2	[c, d]
1980 Jun 29	18:26	2380	2522	S29 W90	M4.2	[c, d]
1980 Jul 1	16:28	2640	2544	S12 W38	X2.5	[c]
1980 Jul 5	22:46	4760	2550	N28 W29	M8.9	[b]
1980 Jul 12	11:19	1400	2562	S14 E56	M4.3	[c]
1980 Jul 14	08:27	4550	2562	S13 E43	X1.1	[c, b]
1980 Jul 21	03:00	2550	2562	S14 W60	M8.0	[c]
1980 Aug 23	21:30	800	2629	N16 W39	M2.1	[b]
1980 Aug 31	12:52	1200	2646	N12 E28	M2.8	[c]
1980 Oct 14	06:15	8040	2725	S09 W07	X3.3	
1980 Nov 5	22:36	1850	2776	N11 E07	M4.0	
1980 Nov 7	04:58	1420	2779	S10 E57	M2.5	
1980 Nov 12	02:52	760	2779	S13 W06	M1.9	
1980 Nov 12	17:05	530	2779	S14 W11	M1.4	[b]
1980 Nov 18	14:56	1430	2779	S10 W90	M3.0	[c, d]
1980 Nov 19	04:39	545	2779	S10 W90	M9.0	[d]
1980 Nov 19	05:45	2730	2779	S10 W90	M6.0	[b, c, d]
1980 Nov 22	05:38	230	2793	N11 W02	C9.0	
1984 Apr 26	09:04	1830	4474	S09 E34	M2.5	
1984 May 2	19:26	1950	4474	S11 W58	M3.0	
1984 May 5	18:24	6170	4474	S11 W90	M7.5	[c, d]
1984 May 19	21:56	7930	4492	S10 E67	X4.1	
1984 May 20	01:29	2100	4492	S10 E64	M2.9	
1984 May 20	03:02	3150	4492	S08 E64	M4.6	[b]
1984 May 20	22:54	4740	4492	S09 E52	X10.	[a]
1984 May 21	18:10	1130	4492	S08 E42	C8.5	
1984 May 22	15:02	3250	4492	S09 E26	M7.0	
1985 Jan 20	20:52	2940	4617	S09 W24	M4.1	[a]
1985 Jan 23	07:33	780	4617	S12 W59	M1.3	
1985 Apr 24	01:52	560	4647	N03 E27	C8.8	
1985 Jul 2	21:26	3330	4671	S15 E56	M4.5	[a]

[a] Rise phase not recorded.
[b] Upflow velocity or turbulent velocity increasing at the flare beginning.
[c] Weak plasma upflow recorded.
[d] limb.

generally predict that most of the plasma is moving and the blueshifted component dominates the stationary component (Cheng *et al.* 1983). This is not supported by the observations.

The time history of parameters derived from the two-component spectral fitting are shown for the 1980 April 8 (importance 1B/M4) flare in Figure 4. Displayed are the calcium light curve, the electron temperature, the emission measures of the stationary (EM_S) and blueshifted (EM_B) components, and the "turbulent velocity" of the stationary component computed from the line width of the stationary component after subtracting the thermal broadening

$$v_T = [2k(T_D - T_e)/m]^{1/2} , \quad (4)$$

where k is the Boltzmann constant, m is the atomic mass of the ion responsible for the line emission, and T_D is Doppler temperature given by

$$T_D = \frac{mc^2}{2k}\left(\frac{\Delta\lambda_S}{\lambda_S}\right)^2 . \quad (5)$$

Also displayed is the mean upflow velocity computed as

$$v_U = c(\lambda_S - \lambda_B)/\lambda_S , \quad (6)$$

where c is the speed of light. The error bars in Figure 4 and the uncertainties quoted elsewhere in the text are 1 σ statistical errors (see § IV). The plasma upflow is observed for this flare from nearly the beginning of the impulsive phase. The intensity ratio of the blueshifted component to the stationary component has a maximum value of $I_B/I_S = 0.7 \pm 0.16$. This spectrum is plotted in Figure 2.

After the time of the maximum calcium total count rate, only a one-component model is applied. The "switching off" of the blueshifted component results in an artificial discontinuity of some of the fitted quantities. The emission measure of the stationary component increases by $\sim$10% and the turbulent velocity of the stationary component (v_T) increases by $\sim$40 km s^{-1} at this time. The total emission measure $EM_S + EM_B$, however, does not show a discontinuity.

The time history of the fitted parameters for the 1980

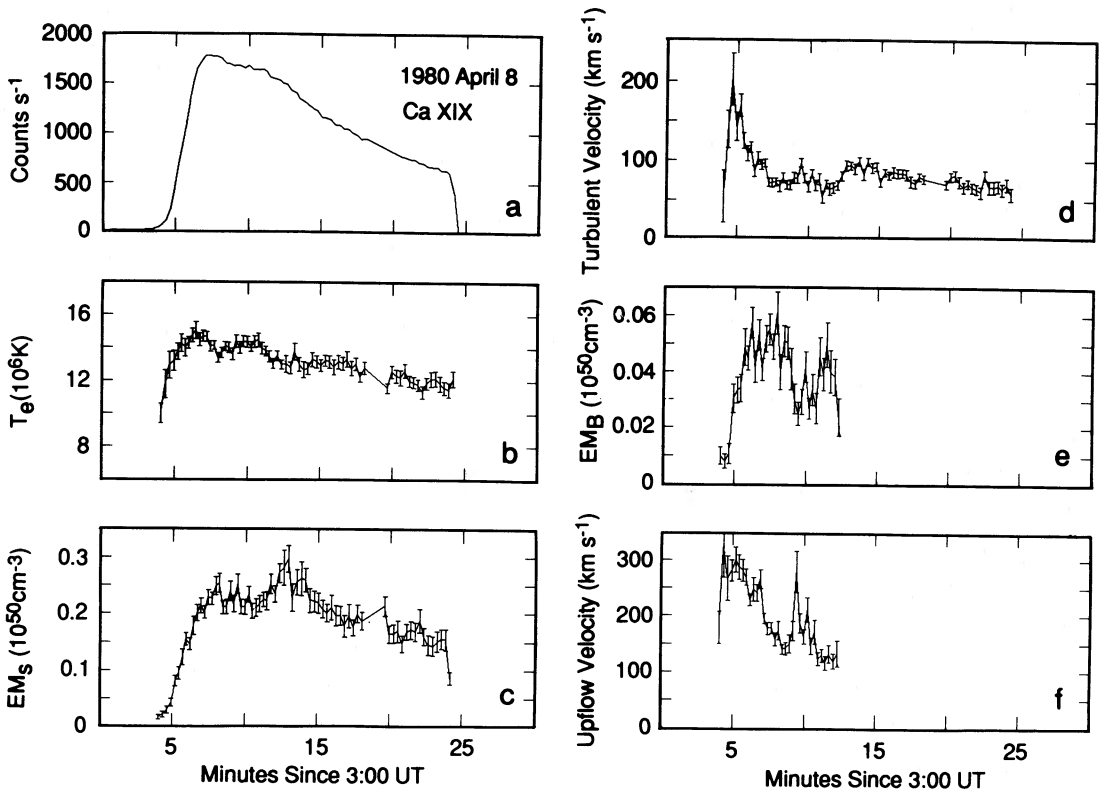

FIG. 4.—Time history of flare parameters derived from BCS Ca XVIII–XIX data for the flare on 1980 April 8. Displayed are (*a*) the total counting rate, (*b*) the electron temperature, (*c*) the emission measure of the stationary plasma, (*d*) the turbulent velocity determined from the width of the stationary component after subtracting the thermal broadening, (*e*) the emission measure of moving plasma, and (*f*) the mean upflow velocity. The error bars represent 1 σ uncertainties determined from the fitting procedure. At 3:12:38 UT the two-component fitting was "switched off" and one-component fits were applied until the end of the flare.

October 14 flare (importance 3B/X3) is shown in Figure 5. The maximum observed intensity ratio of the blueshifted component to the stationary component was $I_B/I_S = 0.38 \pm 0.03$. This flare produced very high counting rates in the BCS and the plasma upflow was observed to last for more than 8 minutes. It is also a good example to illustrate the time history of the fitting parameters for iron. Note that at 6:18:17 UT the second component was artificially switched off. A comparison of the calcium and iron results is discussed in § III*e*.

Eight of the flares analyzed were observed on the solar limb. For most of them only small asymmetries can be detected in the spectral line profiles, suggesting that the plasma motion is nearly vertical (see Antonucci *et al.* 1982, 1984). However, for the 1980 November 19 flare at 04:35 UT a significant blueshifted component is detected with $I_B/I_S = 0.25$ to 0.35 and upflow velocity $v_U = 260$–360 km s^{-1}. Presumably in this flare the directed plasma motions are occurring in a loop which is significantly inclined relative to the vertical direction.

Five of the flares, located on the disk, also showed a very small asymmetry of the line profiles. This may be caused by the fact that the observing line of sight was almost perpendicular to the direction of the plasma upflow, or it may be the result of a much more gradual heating of the flare plasma.

b) Blueshifted Component during Decay Phase

The blueshifted component is often interpreted as a signature of chromospheric evaporation which is associated with the impulsive or heating phase of the flare. For most flares the blueshifted component disappears when, or shortly after, the flare reaches its maximum intensity. However, for several big flares (e.g., 1980 October 14, 1980 May 21), the two-component algorithm continues to fit a weak, although statistically significant, blue-shifted component following the flare maximum and during the decay phase. The upflow velocities are then ~100–150 km s^{-1} and the intensity ratio of the blueshifted to the stationary component is ~0.1–0.15. This phenomenon was also discovered by Gunkler *et al.* (1984), who analyzed the BCS Ca XIX spectra for the flare of 1980 June 24 by means of a different technique.

The statistical significance of one compared to two components during the decay phase of the 1980 May 21 flare was evaluated. With the use of the method of Avni (1976) and Cash (1976), already applied in § II, the hypothesis that the blueshifted intensity was equal to zero was tested. In many spectra the single-component fits were not acceptable at the 0.01 significance level and therefore, forced the acceptance of the two-component model.

The upflow velocity during the flare decay may be the result of many magnetic loops which are heated sequentially, since these observations have occurred for large flares. This may be evidence of "gentle evaporation" (Zarro and Lemen 1988), which is driven by thermal conduction downward from the heated flare plasma.

We cannot rule out the possibility that the weak blueshifted features sometimes detected in the decay are simply an artifact, perhaps caused by an error in the spectral model or the instrument resolution function. Further, the typical velocities detected during the decay phase are near the detection limit for the BCS. The FWHM of the Voigt profile which corresponds to the wavelength response function of the BCS Ca XIX spec-

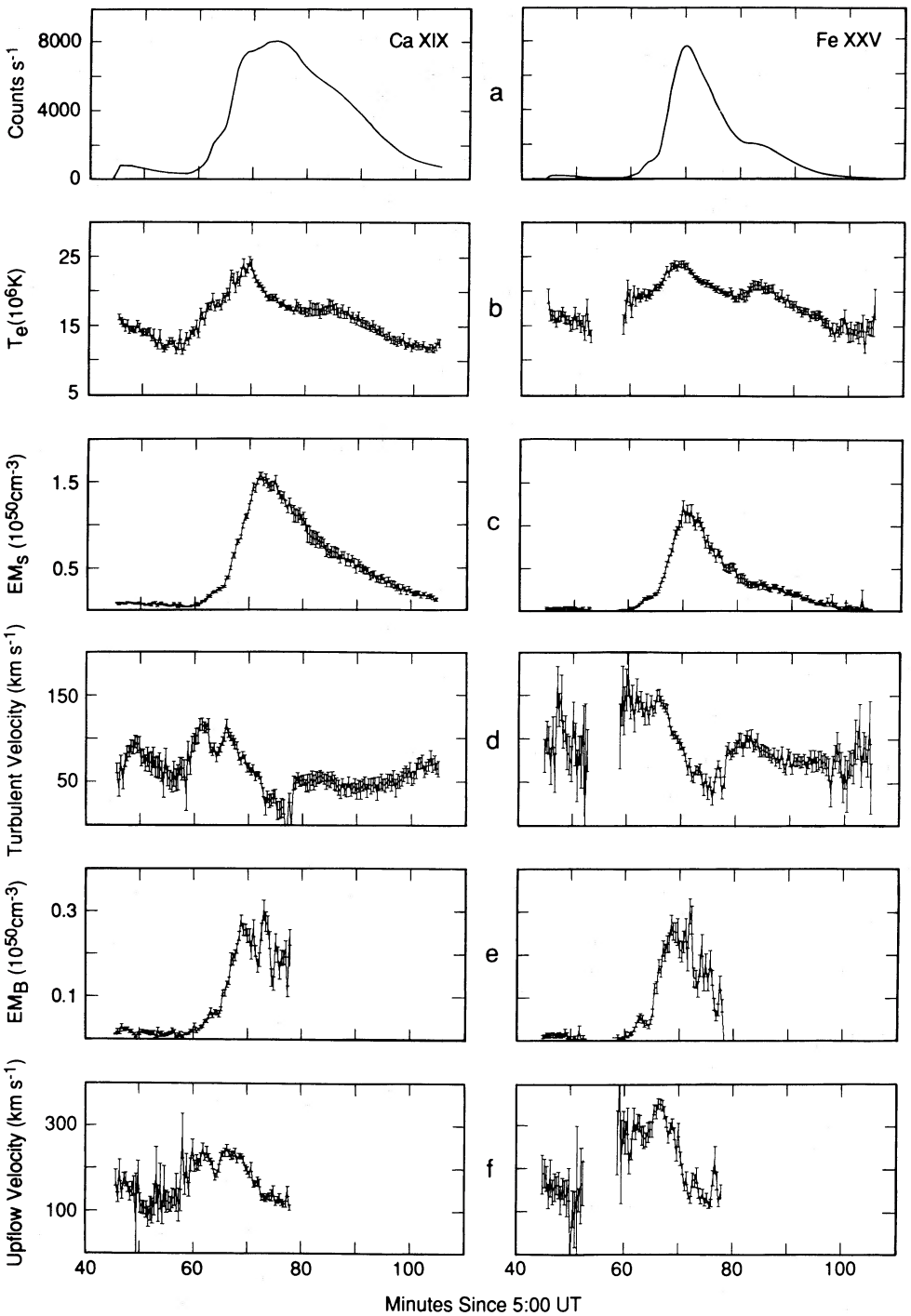

FIG. 5.—(*a-f*) Time history of the flare parameters (as in Fig. 4) obtained during the 1980 October 14 flare from Ca XVIII–XIX (*left panels*) and Fe XXII–XXV (*right panels*) data. Each of the displayed parameters has the same scale on both panels, which allows to compare directly results from calcium and iron spectra. The two-component fitting was "switched off" at 6:18:17 UT. For this large flare, a dead time correction has been applied in the calculation of the emission measures.

trometer is 0.918 mÅ, which corresponds to a velocity shift of $\approx$90 km s^{-1}, making it difficult to detect upflow velocities which are smaller than this.

c) *Stationary Component Nonthermal Line Broadening*

From the above examples and other investigated flares emerge some general trends for the nonthermal or "turbulent" broadening of the stationary component, v_T (see eq. [4]). Nonthermal refers to the broadening which is in excess of that due to the instrumental profile and thermal broadening for a plasma with a temperature T_e determined by the spectral fitting. For many flares the turbulent line broadening, v_T, is observed to increase at the beginning of the impulsive phase. The maximum value of v_T typically reaches 120–140 km s^{-1}, at the same time or 1–3 minutes before the maximum is reached in the electron temperature. The nonthermal line broadening often decreases with a constant rate until it reaches its minimum value of 40–80 km s^{-1} at about the time when the total emission measure is at its maximum. These results are

similar to results discussed by Doschek *et al.* (1980), Antonucci *et al.* (1984), Doschek *et al.* (1986). Note that in the case of the 1980 October 14 X3.3 flare (Fig. 5) there are two maxima of v_T during the impulsive phase, corresponding to two increases in the electron temperature. Jakimiec *et al.* (1986) suggest that this type of correspondence may be due to coupling between turbulent motions and the release of flare energy.

We have referred to the symmetric line broadening as turbulent broadening, however, some authors think it may not be necessary to introduce a turbulent mechanism to explain the excess line broadening (Doschek *et al.* 1986). In fact, synthetic spectra generated from the results of a numerical model of a one-dimensional single loop with no turbulence (Mewe *et al.* 1985) show line widths which far exceed that expected for an isothermal plasma. The reason is that there is a distribution of velocities over the whole loop length. When emission over the entire loop is integrated, the resultant profiles can appear highly broadened yet symmetric. This interpretation is consistent with the view adopted by Doyle and Bentley (1986) who analyzed impulsive phase BCS Ca XIX spectra for several flares. They reported the presence of several directed mass flows early in the impulsive phase which eventually became blended into one profile.

At the very beginning of some flares the spectral fitting algorithm gives a maximum value of v_T greater than 200 km s^{-1}, accompanied by a rather weak blueshifted component. An example of this situation was obtained with the flare observed on 1980 November 5 at 22:33:24 UT. In these cases, although the line profile is almost symmetric, it is very likely that the strong broadening is caused by a superposition of a stationary component and a blueshifted component with comparable intensities. One should interpret carefully spectra which are broad and nearly symmetric, especially at the very beginning of the flare. Statistically it may be acceptable to interpret such spectra solely in terms of turbulent motions, but in fact a component emitted by upflowing plasma may be present, although not resolvable (e.g., with the mean velocity less than 90 km s^{-1}; see § III*b*).

Finally, in none of the 40 flares studied did the value of v_T reach a null value during the decay phase. In fact, in some cases v_T is observed to increase ~10–30 minutes following the flare peak. The typical postflare values of the velocity seen both in calcium and iron spectra, in the range 40–80 km s^{-1}, are close to values found in Ca XIX spectra recorded by the SOLFLEX spectrometer on the *P78-1* mission (Doschek *et al.* 1980; Feldman *et al.* 1980). They also appear to be in agreement with active region results obtained for Mg XII spectra (Grineva *et al.* 1973) and for Mg XI spectra (Saba and Strong 1986). However, turbulent velocities measured in iron spectra are at least the same or higher than those measured in calcium spectra. The same relation is also true for the upflow velocities. As the iron spectra are representative of hotter plasma, this means that hotter plasma moves faster.

d) Relationship between Turbulent and Upward Motions

The time relationship between the directed upward motions and the turbulent motions measured in the symmetric broadening of the stationary component during flare development has been considered. In 12 flares the time of the maximum upflow velocity corresponded to the time of the maximum turbulent velocity to within ~15–25 s, which is equal to the integration time used in the analysis. For five of these flares this correlation is even stronger—both velocities show similar behavior over a period of 3–5 minutes. The best example of this correlation was observed for the 1980 May 21 X1.4 flare. Figure 6 shows the turbulent velocity v_T plotted as a function of the upflow velocity v_U. In this case the correlation is linear with a slope of ~0.35. The other four flares had slopes which varied between ~0.35 and 0.55.

In most flares the sensitivity of the BCS is not sufficient to allow us to decide whether the upward bulk motions or the turbulent motions begin first. However, in two flares (1984 May 20, 02:59:19 UT, Δt = 15.36 s and 1980 April 8, 03:04:04 UT, Δt = 18.04 s) it is possible to observe a significantly blueshifted component at the very beginning of the flare when the turbulent velocity v_T, as measured from the broadening of the stationary component, is only ~55 km s^{-1} (Fig. 7). This value

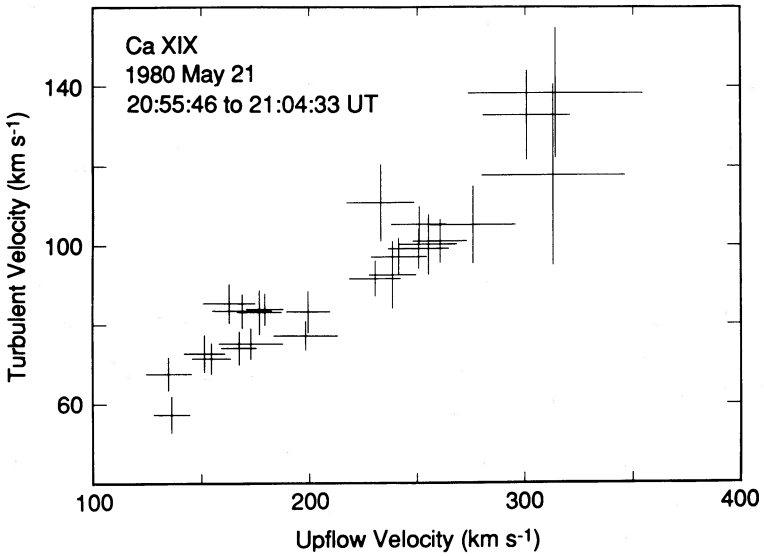

FIG. 6.—The correlation of the turbulent and upflow velocities observed in Ca XVIII–XIX during the rise phase of the 1980 May 21 flare, between 20:55:46 and 21:04:33 UT. Later time points are in the lower left-hand part of the diagram. Crosses indicate 1 σ errors.

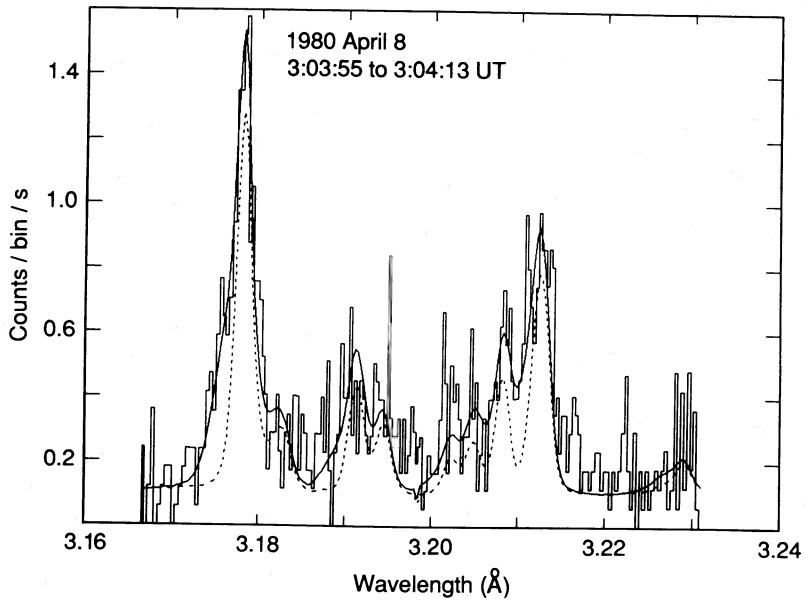

FIG. 7.—A Ca XVIII–XIX spectrum (*histogram*) and a two-component fit (*solid line*) obtained early in the impulsive phase for the 1980 April 8 flare at 3:04:04 UT (integration time is 18 s). The stationary component is represented by a dashed curve. This fit shows a moderately large upflow velocity ($v_U = 178$ km s^{-1}) but a small turbulent velocity ($v_T = 55$ km s^{-1}). The intensity ratio of the blueshifted to the stationary component is 0.57 ± 0.23.

of v_T is typical both for an active region (Saba and Strong 1986) and for the decay phase of most flares, but is unusually small for the impulsive phase of a flare. This observation could be interpreted as evidence for plasma upflow preceding flare turbulence. We have not found, however, a convincing evidence of a directed motion of the entire soft X-ray source (Antonucci *et al.* 1985).

e) Temperature of Moving Plasmas

Since the blueshifted component of the helium-like forbidden line tends to blend with the dielectronic satellite *k* or *j* lines in Ca XVIII–XIX or Fe XXIV–XXV spectra, it is necessary to apply the two-component model to calculate accurately the line intensities and estimate the electron temperature during the flare rise phase. As discussed earlier, for the spectral fitting it is assumed that the mean electron temperatures of the stationary and moving plasmas are the same. The reasons for this assumption are that the blueshifted components of the satellite lines are blended with other nearby satellites (in the notation of Gabriel 1972: lines *a*, *d*, and *r* in calcium; lines *k* and *r* in iron) and the dielectric satellites are themselves weaker than the resonance line. Thus the intensity of the dielectronic line blue-component cannot be satisfactorily measured and the temperature cannot be estimated for the two components independently. On the other hand, the numerical models of a one-dimensional flare loop heated at the top (Pallavicini *et al.* 1983) indicate that plasma with upflow velocities greater than ~ 250 km s^{-1} can be cooler—on average by up to 5×10^6 K—than the plasma located at the top of the loop. Thus it is essential to derive both temperatures independently from observations.

We propose that temperature information about the blueshifted component can be determined from comparisons of *simultaneously* obtained calcium and iron spectra (Fludra 1987). The ratio of the theoretical intensities of the resonance lines of calcium to iron, I(Ca)/I(Fe), is a monotonically decreasing function of temperature. This property can be used to compare the mean temperatures of the blueshifted and stationary components. If the inequality

$$I_B(\mathrm{Ca})/I_B(\mathrm{Fe}) < I_S(\mathrm{Ca})/I_S(\mathrm{Fe}) \qquad (7)$$

is found to be consistent with the observations, it would imply that the mean temperature of the upflowing component is greater than the mean temperature of the stationary component. The left-hand side of equation (7) represents the ratio of the intensities of the resonance lines of the blueshifted component in calcium and iron. The right-hand side represents the same ratio for the stationary component. The inequality expressed by equation (7) is independent of the relative sensitivities of the BCS Ca XIX and Fe XXV channels and of the values of the elemental abundances assumed for calcium and iron, provided that the relative abundance of calcium to iron in the moving plasma is the same as in the stationary plasma.

The time histories of I_B(Ca)/I_B(Fe) and I_S(Ca)/I_S(Fe) are plotted in Figure 8 for the rise phase of the 1980 October 14 flare between 5:59 and 06:10 UT. For most of the time the two quantities are equal to each other, to within the 1 σ uncertainties of the measurements. However, the ratio I_B(Ca)/I_B(Fe) is systematically lower and when the upflow velocity is the highest, the difference is $\sim 2\ \sigma$. This might indicate that the temperature of the upflowing plasma is greater by up to 3×10^6 K than the temperature of the stationary plasma. This suggests that the initial deposition of energy might have occurred close to the flare footpoints. This result was obtained for several other flares as well, and it supports results of Antonucci *et al.* (1987), who came to a similar conclusion by comparing numerical flare models with BCS Ca XIX spectra. As far as we know, our attempt to characterize the temperature of the upflowing component is the first one made directly from X-ray observations by simultaneous using of calcium and iron spectra. Antonucci *et al.* (1984) indirectly inferred the average value of T_e^B for the impulsive phase from requirements of mass and energy conservation and obtained the opposite relation of temperatures.

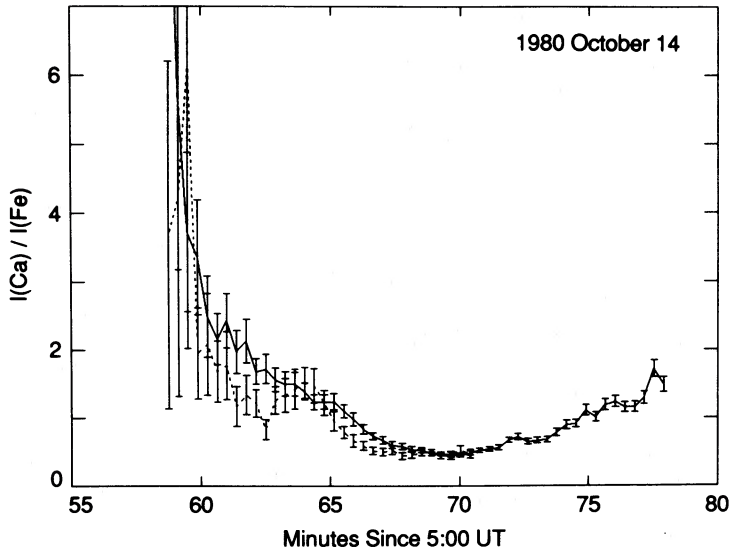

FIG. 8.—The resonance line intensity ratio of Ca XIX to Fe XXV for the two components determined during the rise phase of the 1980 October 14 flare. This ratio is a monotonically decreasing function of electron temperature. The solid curve connects stationary component data points, and the dashed curve connects blueshifted component data points. The error bars represent 1 σ uncertainties determined from the fitting procedure.

Since the plasma is indeed multi-thermal (see Jakimiec *et al.* 1984), both components may possess different distributions of the differential emission measure. The current analysis, which uses only two lines, would not be very sensitive to it. A more realistic interpretation could be made if the blue component were observed in several different ions representing a broader range of temperatures. One of the several known techniques (see Fludra and Sylwester 1986; Bruner *et al.* 1989) should then be used to calculate the distribution of the emission measure over temperature.

The fact that for times close to flare beginning $I_B(\mathrm{Ca})/I_B(\mathrm{Fe}) < I_S(\mathrm{Ca})/I_S(\mathrm{Fe})$ suggests that the observations are consistent with the proposition that the moving plasma is hotter than the stationary plasma. However, as the difference in mean temperature is less than 3 million K and is within 2 σ error, it allows one to use the original assumption that the electron temperatures for the two components may be regarded as equal to within the statistical uncertainties. The fitting algorithm is not significantly biased because of this assumption.

If the real mean temperatures of the moving and stationary plasma were different at some moment during a flare, then the emission measures calculated by our method at this moment should be corrected. For example, if $T_B = 18$ MK, $T_S = 15$ MK, then the actual ratio $\mathrm{EM}_B/\mathrm{EM}_S$ would be lesser by a factor of 1.6 than calculated with the assumption $T_B = T_S$. The ratio would be *greater* by the same factor if the mean temperatures were $T_B = 15$ MK, $T_S = 18$ MK.

IV. DISCUSSION

An improved method for fitting asymmetric soft X-ray spectra has been presented. This method statistically determines both the fitting parameters, which represent the physical condition of the flaring plasma, and their uncertainties. We interpret the plotted error bars and the quoted uncertainties as 1 σ errors. This interpretation was experimentally checked in the following manner. Assume that P^* is the value of a parameter that minimizes χ^2, denoted as $\chi^2_{\min}$, and that σ is the statistical error of the parameter. The interpretation of σ is that it is the value by which P^* must be varied to cause an increase of the χ^2 statistic from $\chi^2_{\min}$ to $\chi^2_{\min} + 1$ when all other parameters but the one of interest are allowed to vary. For linear models this procedure gives the probability of 0.68 that the true value of the parameter is in the interval $(P^* - \sigma, P^* + \sigma)$. The two-component spectral fitting is a nonlinear model and therefore, the probability has been determined by a numerical simulation. Three hundred two-component spectra were generated theoretically for a set of typical values of the resonance line widths, intensities, and upflow velocities, to which statistical noise was added. The two-component spectral fitting model was applied to each spectrum. The best-fitted parameters were investigated individually to determine what value of σ was required to increase the χ^2 statistic to $\chi^2_{\min} + 1$. The probability, to within $\pm 3\%$ error, that the difference between the assumed and calculated parameter value is less than σ was found to be 0.68, and the probabilities of 0.90 and 0.99 were found to correspond to 1.6 σ and 2.6 σ, respectively, as would be expected for a linear model. Thus, all quoted uncertainties using the method presented can be interpreted as 1 σ errors.

The fitting method has been used to interpret the soft X-ray spectra as being emitted from plasma which is subject to directed motions, and from stationary plasma in a turbulent state. However, it may not be necessary to introduce turbulent motions to explain the line broadening of the stationary component, although, it seems likely that the deposition of a large amount of energy during the impulsive phase is bound to disturb or even tangle the magnetic field lines which could subsequently give rise to nonthermal ion motions. The alternative view is that the broadening of stationary component lines is the result of the superposition of emissions from upflowing plasmas distributed over a flare loop or from many individual loops. If such were the case, the results of the two-component spectral model would be interpreted as representing different ranges of the upflow velocities. However, if this view is correct a stronger variation of "turbulent velocities" would be expected across the solar disk. Since observations show that both limb and disk flares have similar broadening of the stationary component, we conclude that while it is probable that

upflowing plasma is partially responsible for the symmetric broadening of the stationary component, it is also caused by turbulent ion motions.

We note that the choice of a Gaussian distribution to represent the shape of the blueshifted component and the constraint that its Doppler width is given by $\Delta\lambda_B = K(\lambda_S - \lambda_B)$ are somewhat arbitrary choices. A different parametric function is possible. However, we note that the model we present is statistically adequate to describe the BCS spectra and that the method can be applied in an automatic fashion to many data sets to determine the systematic behavior of various plasma parameters. This approach has been applied to 40 flares observed by the *SMM* and several important results have emerged.

1. There is an inherent uncertainty in characterizing the blueshifted component. Although it has been determined that $K = 1$ in equation (1) is adequate to fit most spectra, no special significance should be attached to this value. Other values of K, between 0.6 and 3.0, are often, but not always permitted. The main consequence of choosing a larger value of K would be to increase the intensity ratio of the upflowing component to the stationary component. This suggests that it is possible to obtain even higher proportion of the moving to stationary plasma, thus getting a closer agreement between results of hydrodynamic modeling and observations, by further relaxing the constraints imposed on the shape of the moving component. Results of such a study will be published in a future paper.

2. The blueshifted component is broader than the stationary component. This is consistent with the assumption that the blueshifted component represents the emission from the upflowing plasma which contains a broad range of upflow velocities, or indicates that the turbulent motions of the upflow plasma may be larger than that of the stationary component.

3. The turbulent and upflow velocities are generally weakly correlated except in a few flares. For two flares it was possible to determine that the upflow began before the turbulent velocity increased above its preflare value. Possibly if the instrument sensitivity were greater, this time sequence might be found in other flares.

4. By using the calcium and iron results it is possible to infer the relative temperatures of the stationary and upflowing plasma. This can be accomplished only in large, relatively hot flares which produce an adequate signal to noise in the iron spectra. Perhaps surprisingly, this study indicates that the mean temperatures of the upflowing and stationary plasma agree to within the 2 σ uncertainties of the measurements, although there is an indication that at the beginning of the rising phase, the temperature of the upflowing plasma may be systematically *higher*. This may imply that the flare energy is not deposited at the top of flaring loops, but somewhere low in the loop (although not necessarily at the footpoints). As noted above, however, this conclusion may be valid only for large, hot flares, since only these provide adequate signal for investigation.

5. The presence of turbulent motions is detected late in the flare decay phase for every flare studied (a similar result to that found by Doschek *et al.* 1980 and Feldman *et al.* 1980). In some cases there is evidence for continued plasma upflows during the gradual phase. This might be the signature of "gentle evaporation" which is caused by the downward conduction of heat from the plasma which was evaporated to the top of the loop during the rise phase (Zarro and Lemen 1988). This effect is mostly observed in big flares both in calcium and iron spectra. However, we cannot rule out the possibility that the second component during the decay phase is the result of a systematic disagreement between the data and the assumed model.

Finally, we note the possibility of improved measurements of plasma motions during the next solar maximum using the Bragg Crystal Spectrometer which is to be carried on the Japanese *Solar-A* mission in 1991. The *Solar-A* spectrometer will have comparable wavelength resolution to the *SMM* spectrometers, but will have approximately an order of magnitude higher sensitivity in Fe XXVI, Fe XXV, Ca XIX, and S XV. Such sensitivity will make possible studies earlier in the rise phase, which is crucial to increased understanding, with a broader range of temperature diagnostics.

The authors wish to thank J. L. Culhane for his encouragement and useful suggestions concerning this paper. A. F. acknowledges a grant from the UK Foreign and Commonwealth Office and expresses his sincere thanks to the British Council for their assistance. Support for this paper was also provided by the UK Science and Engineering Research Council, NASA contract NAS5-28713, and the Lockheed Independent Research Program. The soft X-Ray Polychromator instrument was build by a consortium of three groups: the Lockheed Palo Alto Research Laboratory (L. W. Acton), the UCL Mullard Space Science Laboratory (J. L. Culhane) and the Rutherford Appleton Laboratory (A. H. Gabriel).

REFERENCES

Antonucci, E., Dennis, B. R., Gabriel, A. H., and Simnett, G. M. 1985, *Solar Phys.*, **96**, 129.
Antonucci, E., Dodero, M. A., Peres, G., Serio, S., and Rosner, R. 1987, *Ap. J.*, **322**, 522.
Antonucci, E., *et al.* 1982, *Solar Phys.*, **78**, 107.
Antonucci, E., Gabriel, A. H., and Dennis, B. R. 1984, *Ap. J.*, **287**, 917.
Avni, Y. 1976, *Ap. J.*, **210**, 642.
Bely-Dubau, F., *et al.* 1982, *M.N.R.A.S.*, **201**, 1155.
Bruner, M. E., Brown, W. A., Fludra, A., Lemen, J. R., Mason, H. E., and McWhirter, R. W. P. 1989, in preparation.
Bruner, M. E., Crannel, C. J., Goetz, F., Magun, A., and McKenzie, D. L. 1988, *Ap. J.*, **334**, 494.
Cash, W. 1976, *Astr. Ap.*, **52**, 307.
Cheng, C. C., Oran, E. S., Doschek, G. A., Boris, J. P., and Mariska, J. T. 1983, *Ap. J.*, **265**, 1090.
Culhane, J. L., *et al.* 1981, *Ap. J. (Letters)*, **244**, L141.
Doschek, G. A., Feldman, U., Kreplin, R. W., and Cohen, L. 1980, *Ap. J.*, **239**, 725.
Doschek, G. A., *et al.* 1986, in *Proc. SMM Workshop, Energetic Phenomena on the Sun*, ed. M. R. Kundu and B. Woodgate (NASA CP-2439), p. 4-1.
Doyle, J. G., and Bentley, R. D. 1986, *Astr. Ap.*, **155**, 278.
Feldman, U., Doschek, G. A., Kreplin, R. W., and Mariska, J. T. 1980, *Ap. J.*, **241**, 1175.
Fludra, A., and Sylwester, J. 1986, *Solar Phys.*, **105**, 323.
Fludra, A. 1987, Ph.D. thesis, Wroclaw University.
Gabriel, A. H. 1972, *M.N.R.A.S.*, **160**, 99.
Grineva, Yu. I., Karev, V. I., Korneev, V. V., Krutov, V. V., Mandelstam, S. L., Vainstein, L. A., Vasilyev, B. N., and Zhitnik, I. A. 1973, *Solar Phys.*, **29**, 441.
Gunkler, T. A., Canfield, R. C., Acton, L. W., and Kiplinger, A. L. 1984, *Ap. J.*, **285**, 835.
Hata, J., and Grant, I. P. 1984, *M.N.R.A.S.*, **211**, 549.
Jacobs, V. L., Davis, J., Kepple, P. C., and Blaha, M. 1977, *Ap. J.*, **211**, 605.
Jacobs, V. L., Davis, J., Rogerson, J. E., Blaha, M., Cain, J., and Davis, J. 1980, *Ap. J.*, **239**, 1119.
Jakimiec, J., Fludra, A., Lemen, J. R., Dennis, B. R., and Sylwester, J. 1986, *Adv. Space Res.*, **6**, 191.
Jakimiec, J., Sylwester, J., Lemen, J. R., Mewe, R., Bentley, R. D., Fludra, A., Schrijver, J., and Sylwester, B. 1984, *Adv. Space Res.*, **4**, 203.
Korneev, V. V., Krutov, V. V., Madelstam, S. L., Urnov, A. M., and Zhitnik, I. A. 1979, *Solar Phys.*, **63**, 319.

Lemen, J. R., Phillips, K. J. H., Cowan, R. D., Hata, J., and Grant, I. P. 1984, *Astr. Ap.*, **135**, 313.
Mewe, R., Lemen, J. R., Peres, G., Schrijver, J., and Serio, S. 1985, *Astr. Ap.*, **152**, 229.
Pallavicini, R., Peres, G., Serio, S., Vaiana, G., Acton, L. W., Leibacher, J., and Rosner, R. 1983, *Ap. J.*, **270**, 270.
Saba, J. L. R., and Strong, K. T. 1986, *Adv. Space Res.*, **6**, 37.
Zarro, D. M., and Lemen, J. R. 1988, *Ap. J.*, **329**, 456.

R. D. BENTLEY and A. FLUDRA: Mullard Space Science Laboratory, Holmbury St. Mary, Dorking, Surrey RH5 6NT, England, UK

J. JAKIMIEC: Astronomical Institute, Wroclaw University, ul. Kopernika 11, 51-622 Wroclaw, Poland

J. R. LEMEN: Lockheed Palo Alto Research Laboratory, Department 91-30, Building 255, 3251 Hanover Street, Palo Alto, CA 94304

J. SYLWESTER: Space Research Centre, ul. Kopernika 11, 51-622 Wroclaw, Poland